

Brillouin scattering study of transverse elastic waves in the α , incommensurate and β phases of AlPO_4

N. Magneron^{1,a}, Y. Luspin¹, G. Hauret¹, and E. Philippot²

¹ Centre de Recherches sur la Physique des Hautes Températures, Centre National de la Recherche Scientifique, 45071 Orléans, France and Université d'Orléans, 45067 Orléans, France

² Laboratoire de Physicochimie de la Matière Condensée, Centre National de la Recherche Scientifique, 34095 Montpellier, France and Université de Montpellier II, 34095 Montpellier, France

Received: 2 October 1997 / Received in final form: 3 December 1997 / Accepted: 29 January 1998

Abstract. Transverse and pseudo-transverse elastic waves have been studied in several scattering geometries in order to investigate the temperature dependences of C_{66}^E and C_{14}^E over the range 300-1100 K, including the transitions near 860 K. These results complete those on C_{44}^E we have obtained in a previous work. All these constants display discontinuities at the lock-in transition. In the α phase, the results are analysed in term of lowest order couplings between strains (e) and the order parameter (Q). The main features are described by the lowest order biquadratic e^2Q^2 coupling, in particular for C_{44}^E in a large temperature range. However, it appears that a contribution of the next coupling term arises for C_{66}^E below ~ 710 K and that the first two lowest order terms have to be taken into account even just below the lock-in transition in the case of C_{14}^E . The temperature dependence of Q has been deduced and it can be well described in the framework of Landau's theory.

PACS. 64.70.Rh Commensurate-incommensurate transitions – 62.20.-x Mechanical properties of solids – 78.35.+c Brillouin and Rayleigh scattering; other light scattering

1 Introduction

Crystalline SiO_2 (quartz at room temperature) has been widely studied since it is one of the most important crystals used in industry. The ternary aluminium phosphate AlPO_4 (berlinite) is an interesting compound since it displays a polymorphism closely related to that of crystalline SiO_2 . On heating, the same successive phases (quartz α , incommensurate, quartz β , tridymite β and cristobalite β) can be observed in both compounds [1]. At room temperature, the mechanical and electromechanical properties of AlPO_4 have been investigated by ultrasonic methods [2–4] and it was concluded that its performance is expected to be better than that of quartz in ultrasonic device applications [2].

Unlike the case of quartz, the elastic properties of AlPO_4 have been little studied above room temperature. Only a Brillouin determination of the elastic constant C_{33} has been made up to the β phase, but serious difficulties were encountered as a result of an important deterioration of the optical quality of the samples during heating [5].

Recently, we have reported a Brillouin investigation over the range 300-1100 K, including the α -incommensurate- β transitions near 860 K [6]. The excellent optical quality of our samples at room temperature

was only slightly affected by heating. In this study, we have first focused on the elastic constants C_{11}^D and C_{33} for two reasons: (i) these constants can be directly obtained from the velocities of longitudinal waves, (ii) the related Brillouin lines are intense ones. We have also determined the elastic constant C_{44}^E , which is directly related to the velocity of a transverse wave, although the cross-section of the related line was much lower than that obtained for the longitudinal waves.

In this paper, we present further investigations mainly focused on transverse or pseudo-transverse waves in order to complete the results previously reported [6]. In spite of small cross-sections and small frequency shifts of the related lines, we have succeeded in obtaining experimental data in the same temperature range 300-1100 K. In particular, the elastic constants C_{66}^E and C_{14}^E , which were the aim of this new study, have been measured; they are of great importance since, as C_{44}^E , they are expected to yield information about the order parameter.

2 Experimental and crystal data

Brillouin scattering experiments were performed with a pressure scanned, triple passed plane Fabry Perot interferometer (effective finesse 70, resolving power 760 000).

^a e-mail: magneron@admin.cnrs-orleans.fr

The spectra are frequency checked by a Michelson interferometer in parallel. The light source is the $\lambda_0 = 514.5$ nm line of a single frequency Ar-ion laser, the frequency of which is controlled by an iodine cell.

The samples were cut from monocrystals, which were grown by the hydrothermal method as explained in [6].

At room temperature (α phase), AlPO_4 belongs to the same space group $P3_121$ as quartz. The parameters of the primitive hexagonal cell are $a = b = 4.942$ Å and $c = 10.97$ Å [2,7]. There are three formula units per unit cell, as in quartz, but the c -parameter is doubled due to the inequivalence of Al and P atoms.

Near 860 K, AlPO_4 undergoes an “ α - β ” structural transition to a hexagonal phase with space group $P6_222$, which is similar to that occurring in quartz. As in this last compound [8,9], between α and β phases, an inhomogeneous state was observed [10] which can be identified as an incommensurate phase [11]. This incommensurate phase extends on a wider temperature range $T_i - T_c = 3$ K than that observed in quartz (1.3 K), T_i and T_c being the $\beta \rightarrow$ inc. and lock-in transition temperatures respectively. The $\beta \rightarrow$ inc. transition is induced by the condensation of soft modes with wave vector $\mathbf{k}_i = \pm 0.03\mathbf{a}^*$ and equivalent by symmetry.

At room temperature, we have measured the refractive indices at λ_0 and obtained the value $n_a = 1.5276$ and $n_c = 1.5369$. The mass density, deduced from cell parameters at room temperature is $\rho = 2.618$ g cm $^{-3}$.

The elastic constants have been referred to a set of orthogonal X , Y and Z axes with X and Z parallel to a binary and the ternary crystallographic axes of the α phase, respectively.

To compute elastic constants from Brillouin shifts at any temperature, we used the room temperature values of both mass density and refractive indices. There are no data on the temperature dependences of indices and the data on lattice parameters are not sufficiently detailed in the vicinity of the transitions.

Brillouin spectra have been performed only on heating the samples in order to avoid eventual hysteresis at the transitions and optical degradation after a first heating run. Some samples break in the vicinity of the lock-in transition T_c but the blocks are large enough in order that the spectra remain unaltered. The optical quality of the samples is preserved up to the highest investigated temperature. However, after cooling down to room temperature, an increase of the Rayleigh peak is generally observed together with a decrease of the Brillouin lines. Therefore, the same sample was not used in more than one heating run.

3 Brillouin experiments and results

3.1 Brillouin experiments

We used right angle scattering geometry for the experiments; in this case the velocity V of an acoustic wave is related to the corresponding Brillouin frequency shift ν

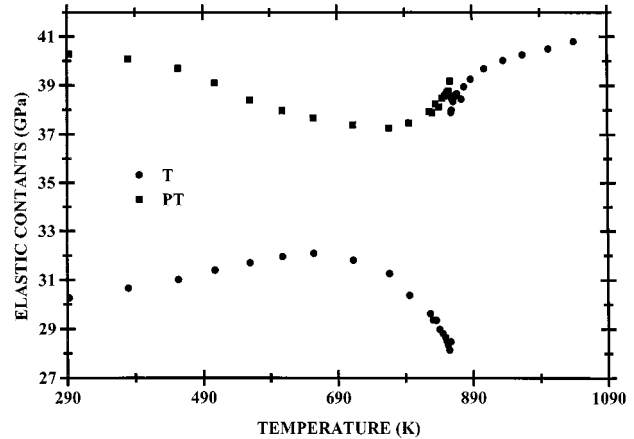


Fig. 1. Temperature dependence of ρV^2 related to the transverse (T) and pseudotransverse (PT) waves in scattering geometries 1 and 2. The wave natures PT and T are exact in the incommensurate and β phases; in the α phase, they can be considered as exact only in the vicinity of room temperature, as explained in the text.

by:

$$V = \lambda_0 \nu / (n_i^2 + n_s^2)^{1/2}$$

where n_i and n_s are the refractive indices for the incident and scattered light beams respectively. The scattering geometries which have been investigated are reported in Table 1.

As recalled in reference [6], the piezoelectricity of the α phase introduces distinctions between elastic constants at constant electric displacement C_{ij}^D and elastic constants at constant electric field C_{ij}^E , except for C_{33} . In the β phase, this distinction only exists for C_{44} .

3.2 Scattering geometries with acoustic wave vector parallel to Y-axis

Within harmonic elasticity, the elastic constant C_{66}^D is expected to be directly obtained from the velocity of the transverse (T) wave in scattering geometry 1. In scattering geometries 1 and 2, the study of line polarizations at room temperature, which were found to agree with the expected selection rules in the α phase, unambiguously allows the assignment of the two weak lines which are recorded beside the intense line related to the pseudo-longitudinal (PL) wave. The T wave related to C_{66}^D have the lowest frequency shift.

The temperature dependences of the “effective” elastic constants ρV^2 for the T and PT (pseudo-transverse) waves are reported in Figure 1. During heating in the α phase, a progressive depolarization of both lines is observed. At a temperature which corresponds to T_c (857 K), a result obtained by the simultaneous recording of the PL wave, the lowest frequency line abruptly disappears. Above T_c , the single line is found to be again full polarized and, according to the selection rules in the incommensurate and β phases, its velocity is related to C_{66} .

Table 1. Characteristics of the investigated scattering geometries. The usual convention for wave vector and polarization direction of the incident and scattered light beams has been used. \mathbf{q} is the acoustic wave vector. L, T, PL, PT are related to the nature of acoustic wave: longitudinal, transverse, pseudo-longitudinal, pseudo-transverse respectively. (*) As explain in text, the line polarizations at room temperature are not preserved on heating. (**) Within the harmonic approximation for elastic properties (no anticrossing induced by anharmonic interactions).

		α -phase			incommensurate and β -phase	
scattering geometries		Acoustic wave vector direction	Acoustic wave nature	Expression of ρV^2	Acoustic wave nature	Expression of ρV^2
1	$(-y+z)[x, -y+z](y+z)^*$	[010]	T ^{*,**}	C_{66}^D	T	C_{66}
2	$(-y+z)[x, x](y+z)^*$	[010]	$\begin{cases} \text{PL}^{**} \\ \text{PT}^{*,**} \end{cases}$	$\begin{cases} \{C_{11}^E + C_{44}^E + [(C_{11}^E - C_{44}^E)^2 + 4C_{14}^{E2}]^{1/2}\}/2^{**} \\ \{C_{11}^E + C_{44}^E - [(C_{11}^E - C_{44}^E)^2 + 4C_{14}^{E2}]^{1/2}\}/2^{**} \end{cases}$	L	C_{11}
3	$(-x+y)[x+y, z](x+y)$	[100]	$\begin{cases} \text{T}_1 \\ \text{T}_2 \end{cases}$	$\begin{cases} \{C_{44}^E + C_{66}^E + [(C_{44}^E - C_{66}^E)^2 + 4C_{14}^{E2}]^{1/2}\}/2 \\ \{C_{44}^E + C_{66}^E - [(C_{44}^E - C_{66}^E)^2 + 4C_{14}^{E2}]^{1/2}\}/2 \end{cases}$	T	C_{44}^E
4	$(-x+z)[(x+z), y](x+z)$	[100]	$\begin{cases} \text{T}_1 \\ \text{T}_2 \end{cases}$	$\begin{cases} \{C_{44}^E + C_{66}^E + [(C_{44}^E - C_{66}^E)^2 + 4C_{14}^{E2}]^{1/2}\}/2 \\ \{C_{44}^E + C_{66}^E - [(C_{44}^E - C_{66}^E)^2 + 4C_{14}^{E2}]^{1/2}\}/2 \end{cases}$	T	C_{66}

In the β phase, the other T wave corresponds to C_{44}^E (inactive in Brillouin scattering for this geometry) which has lower values than those of C_{66} (the results for C_{44}^E [6] are recalled in Figs. 3a and 3b). Therefore, it can be expected that the two modes would cross at some temperature in the α phase, within harmonic elasticity.

Experimentally, however, it turns out that the minimum and the maximum, occurring for $\rho V^2(\text{PT})$ and $\rho V^2(\text{T})$ respectively, obviously indicate an anticrossing-like behaviour between the two modes below T_c . Hereafter, the term anticrossing will be used for sake of simplicity. In fact, such an anticrossing is possible since both modes have the same irreducible representation (E) in common.

In the incommensurate and β phases, the morphic constant C_{14}^E being equal to zero (see Sect. 4), the two modes belong to different irreducible representations (A_2 and E_1). Therefore the anticrossing must disappear, the line must be full polarized (as observed) and $\rho V^2(\text{T})$ is expected to be equal to C_{66} . The curve obtained for C_{66} above T_c shows that pretransitionnal features appear over about 30 K above T_c and then a linear increase with a positive slope takes place at higher temperature.

It is convenient to briefly discuss the possibility of a slight misalignment of the sample. In the α phase it can yield a possible explanation for the existence of a phenomenon similar to an anticrossing, *via* the appearance of non diagonal terms instead of zero ones in the Christoffel equations. In the β phase, such a misalignment must lead to a systematic error in the measurement of elastic constant C_{66} ; however, as emphasized in next Section 3.3, the results are in excellent agreement with those obtained

in scattering geometry 4 in which another crystal cut is used. Furthermore, this hypothesis is inconsistent with the abrupt changes in line polarizations at T_c ; above T_c , these polarizations agree with those which are expected in the incommensurate and β phases in absence of any coupling. Therefore, it can be concluded that such a misalignment, which is always present even when it is small, does not give a significant contribution to the observed anticrossing.

As conclusion, it can be emphasized that scattering geometry 1 does not allow the determination of C_{66}^D in the α phase, probably even at room temperature, owing to the anticrossing. It is interesting to note that this negative point can be avoided in the resonance methods of vibrating plates of parallelepipeds. In quartz for example [12,13], by working with high order harmonics, C_{66}^D has been directly measured from the T mode which is involved in scattering geometry 1. In the same way, the constant C_{14}^E cannot be obtained from the PT wave in scattering geometry 2. It can be thought that the PL wave (scattering geometry 2) would be less affected by an anticrossing with the PT and (or) T waves and then can allow the determination of C_{14}^E . However, this determination needs the knowledge of C_{11}^E , whereas only C_{11}^D is directly measured [6], and the piezoelectricity correction is sufficiently significant to introduce a systematic error in C_{14}^E determination.

3.3 Elastic constants C_{66}^E and C_{14}^E

To determine these constants, the scattering geometries 3 and 4 have been investigated (Tab. 1). They are expected

to give the same results in the α phase and complementary ones in the incommensurate and β phases. The T_2 line in scattering geometry 3 cannot be detected at room temperature but it appears during heating above 690 K. Then, the scattering geometries are also complementary in the α phase. The lines are fully polarized at room temperature, in agreement with the selection rules and no depolarization occurs during heating. The temperature dependences of ρV^2 for the four lines are reported in Figure 2. An excellent agreement can be observed in the α phase between the results of both scattering geometries. At a temperature corresponding to the lock-in transition temperature T_c , as checked by the simultaneous recording of the longitudinal line associated with C_{11}^D , one of the two lines disappears in each scattering geometry, as expected by the selection rules if there is a vanishing of C_{14}^E . In fact, these disappearances can be considered as an experimental proof that C_{14}^E cancels at the lock-in transition. At T_c , discontinuities are observed for the remaining lines. Above T_c , we have $\rho V^2(T) = C_{44}^E$ and $\rho V^2(T) = C_{66}^E$ in scattering geometries 3 and 4 respectively; the results for these constants are in excellent agreement with those obtained for C_{44}^E in [6] and for C_{66}^E in scattering geometry 1 as shown in Figure 3a.

In the α phase, the elastic constants C_{66}^E and C_{14}^E can be successively obtained from experimental results by:

$$C_{66}^E = \rho V^2(T_1) + \rho V^2(T_2) - C_{44}^E$$

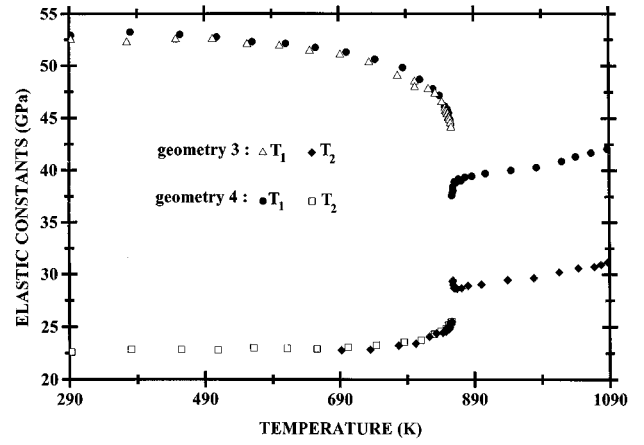
$$C_{14}^E = [(\rho V^2(T_1) - \rho V^2(T_2))^2 - (C_{44}^E - C_{66}^E)^2]^{1/2} / 2$$

making use of values of C_{44}^E determined in [6]. The accuracies are estimated to 5% for C_{66}^E and 7% for C_{14}^E .

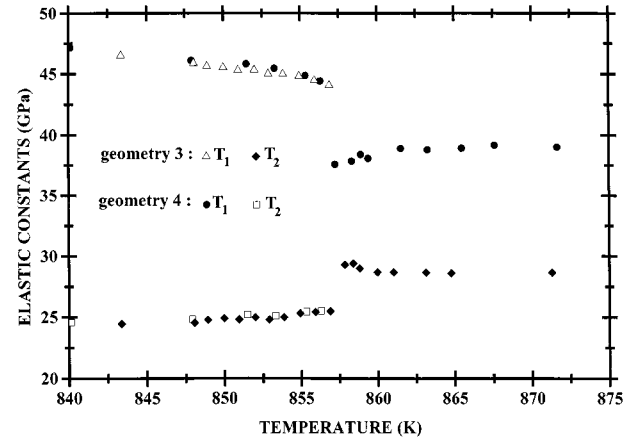
The complete results for C_{66}^E over the temperature range 290-1100 K and the results for C_{14}^E in the α phase are reported in Figures 3 and 4. In Figure 3, we have also reported the curved obtained for C_{44}^E in [6]. In the α phase, C_{66}^E exhibits a non-linear increase up to T_c , where a slight discontinuity occurs. This behaviour of C_{66}^E in the α phase qualitatively resembles that of quartz [12,14]. In this compound, the investigations have been generally made either only in the α phase, or only above T_c . To our knowledge, only one recent investigation has been performed through T_c [15]; a small discontinuity is observed but the evolution below T_c disagrees with previous results [12,14].

In AlPO_4 , above T_c , a pretransitional evolution appears near T_c followed by a linear increase, as already described. It is difficult to compare with the case of quartz since very few results are available in the β phase. A non-linear increase over more than 200 K above T_c has been obtained by Kammer *et al.* [16], whereas more recent results are only given over 8 K above T_c [15,17].

For C_{14}^E , an important decrease of 40% is observed between room temperature and T_c ; at T_c , the constant discontinuously drops to zero. This evolution qualitatively looks like that of C_{14}^E obtained in quartz [8,12,13,18].



(a)



(b)

Fig. 2. (a) Temperature dependence of elastic constants related to transverse waves in scattering geometries 3 and 4. (b) Expanded temperature scale near the transitions.

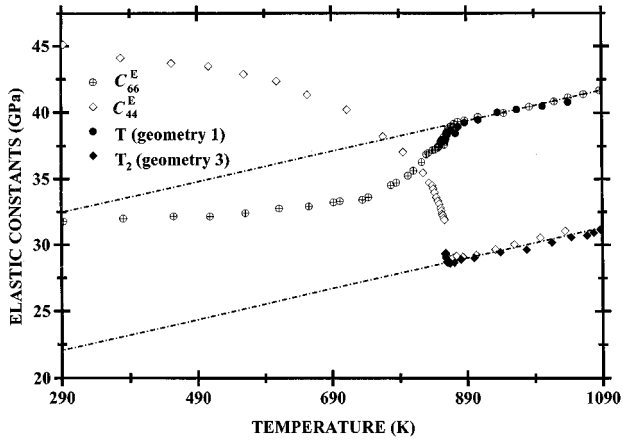
4 Discussion

4.1 Elastic constants C_{44}^E and C_{66}^E

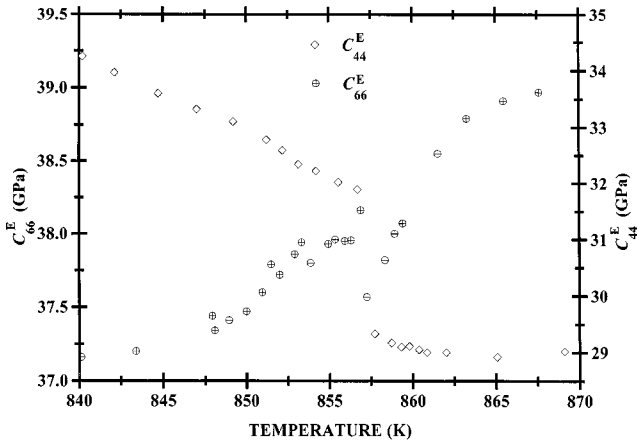
The elastic anomalies near a displacive phase transition are due to interactions between strains, induced by elastic waves, and modes belonging to the soft branch which drives the transition [19], the order parameter Q being related to the modulus of the soft mode amplitude.

The strain e_4 and e_6 being not totally symmetric, the lowest order coupling terms are of the biquadratic type He^2Q^2 and can be written as follows:

$$\sum_{\mathbf{q}, \mathbf{k}} H_j(\mathbf{q}, -\mathbf{q}, \mathbf{k}, -\mathbf{k}) e_j(\mathbf{q}) e_j(-\mathbf{q}) Q(\mathbf{k}) Q(-\mathbf{k}) \quad \text{with } j=4, 6 \quad (1)$$



(a)



(b)

Fig. 3. (a) Temperature dependence of elastic constants C_{66}^E and C_{44}^E . For C_{44}^E the results are those of reference [6]. The extrapolations of the linear variations which hold in the β phase allow the determination of ΔC_{66}^E and ΔC_{44}^E below T_c . Above T_c , the results related to the (T) wave (scattering geometry 1) and (T_2) wave (scattering geometry 3) are also reported for comparison. (b) Expanded temperature scale near the transitions.

where $Q(\mathbf{k})$, which are normal coordinates of modes on the soft branch, are to be taken into account only in the vicinity of the critical wave vectors $\pm\mathbf{k}_i$; $e_j(\mathbf{q})$ is the strain induced by an elastic wave with wave vector \mathbf{q} . As usually, one can consider that $\mathbf{q} \cong 0$.

In the incommensurate phase and below T_c , term (1) gives a static contribution [19] to the anomaly of C_{44}^E and C_{66}^E which is proportional to the order parameter modulus squared:

$$C_{jj}^E = (C_{jj}^E)_0 + 2H_j \sum_i |Q(\pm\mathbf{k}_i)|^2 \text{ with } i = 1, 2, 3$$

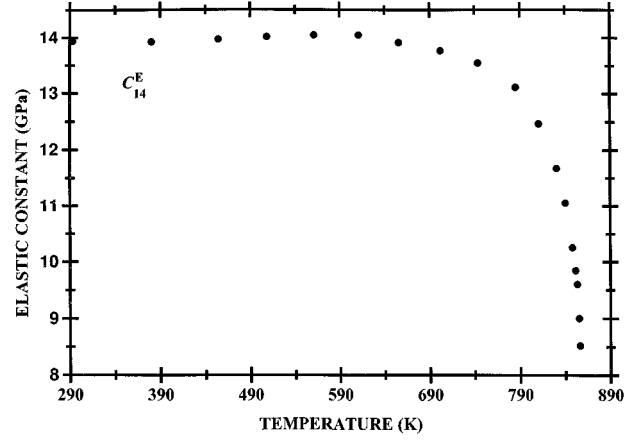


Fig. 4. Temperature dependence of elastic constant C_{14}^E .

where $(C_{jj}^E)_0$ are the bare elastic constants.

In the locked α phase, \mathbf{k}_i is equal to zero. Considering the triple- \mathbf{k} solution adapted for quartz and AlPO₄ [20], there is a common value Q for $|Q(\pm\mathbf{k}_i)|$ which represents the order parameter. Therefore we have:

$$C_{jj}^E = (C_{jj}^E)_0 + h_j Q^2 \text{ with } h_j = 6H_j. \quad (2)$$

Above T_i , in the β phase, we have $Q = 0$ and the elastic constants reduce to the bare ones $(C_{jj}^E)_0$, with $(C_{66}^E)_0 = (C_{66})_0$ since $C_{66}^E = C_{66}^D = C_{66}$. However, it has to be recalled that term (1) can also induce another contribution to elastic constant anomalies which takes place on both sides of the transition at T_i and which are confined on a more or less important temperature range [21]. This contribution can be labelled fluctuation contribution since it only results from fluctuations of the order parameter. In the β phase, near T_i , it can explain, at least partially, the small departure of C_{44}^E and C_{66} from the linear variations which hold at higher temperature. A similar contribution may occur below T_i .

To obtain the anomalous part of C_{44}^E and C_{66}^E below T_i , the linear variations of the elastic constants in the β phase have been extrapolated below T_i and identified with those of the bare ones. Then, considering only the coupling (1) and neglecting the fluctuation contributions, the anomalous parts $\Delta C_{jj}^E = C_{jj}^E - (C_{jj}^E)_0$ are expected to be given by:

$$\Delta C_{jj}^E = h_j Q^2. \quad (3)$$

From experimental results, it is obvious that h_4 is positive and h_6 negative. If h_4 and h_6 are considered to be quasi temperature independent, ΔC_{44}^E and ΔC_{66}^E would be proportional to one another. Unlike ΔC_{44}^E , $|\Delta C_{66}^E|$ exhibits a broad maximum near 720 K, as can be observed in Figure 3a. For the constant C_{66}^E , this fact implies that (3) cannot be satisfied far from the α - β transition, since a normal order parameter has a monotonous variation below the transition temperature [24].

To check the validity of (3) near the transition, a plot of $|\Delta C_{66}^E|$ as function of ΔC_{44}^E is reported in Figure 5.

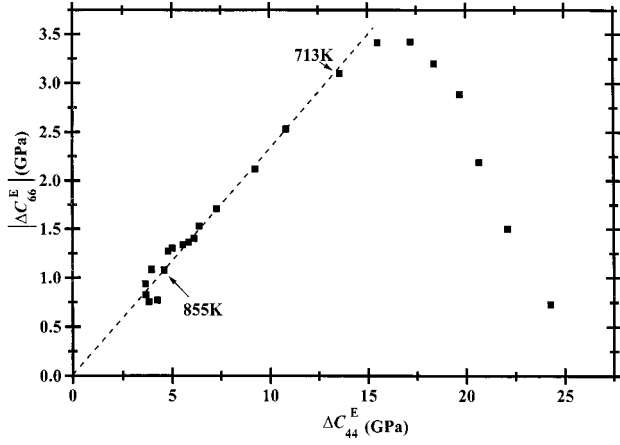


Fig. 5. Plot of $|\Delta C_{66}^E|$ as function of ΔC_{44}^E in the α phase.

Over a temperature range of about 140 K below T_c , a linear portion, whose extrapolation goes through the origin, is effectively observed. This result shows that ΔC_{44}^E and ΔC_{66}^E can be considered as proportional to the order parameter squared in this temperature range. Unlike the case of ΔC_{66}^E , this proportionality may be valid in a wider temperature range for ΔC_{44}^E . Below around 720 K a large deviation from the linear variation occurs. To explain this deviation, we think that it is necessary to put forward higher order coupling terms, allowed by symmetry, such as $M_j e_j^2 Q^4 + \dots$. Below T_i , these terms give additional static contributions to the elastic anomalies which then can be written as:

$$\Delta C_{jj}^E = h_j Q^2 + m_j Q^4 \dots \quad (4)$$

The experimental results for ΔC_{66}^E obviously suggest at least the existence of the first following term $m_6 Q^4$ with a positive coefficient m_6 .

In the β phase, the slopes of the linear variations of C_{44}^E and C_{66} are positive, a result which may be considered as exceptional, since, out of the critical region of a phase transition, the general anharmonicity gives rise to a linear decrease of the elastic constants in most compounds.

Above T_i , it has been pointed out in quartz [17] that the soft branch would interact with the transverse acoustic branch (corresponding to polarization in the (001) plane) for wave vectors in the vicinity of $\pm \mathbf{k}_i$ (along \mathbf{a}^*) and equivalently, leading to a velocity anisotropy for transverse elastic waves with \mathbf{q} small but different from zero. These considerations are also valid in AlPO_4 . Therefore, it is expected that C_{66} , measured for \mathbf{q} along [100] and for \mathbf{q} along [010] (parallel to \mathbf{a}^*), would exhibit different values. The experimental results (scattering geometries 4 and 1 respectively) do not corroborate these predictions, within experimental uncertainties, as it was also concluded in quartz [17]. This can be explain by the low value (~ 0.07) of the q/k_i ratio.

4.2 Elastic constant C_{14}^E

Before the discovery of the incommensurate phase [22], the α - β transition in quartz was attributed to a soft mode at the Brillouin zone centre [23] with B_1 symmetry (or B_2 depending on the choice of the binary axes label). It has been pointed out [19] that a coupling term of the form $Q[(e_1 - e_2)e_4 + e_5 e_6]$ is allowed by symmetry in the β phase. In the α phase, it gives rise to the morphic constants C_{14} , $C_{24} = -C_{14}$ and $C_{56} = C_{14}$ which are proportional to the order parameter.

However, in quartz and quartz-like compounds among which AlPO_4 , the wave vector of the soft modes \mathbf{k}_i being indeed different from zero, such a coupling involving $Q(\mathbf{k}_i)$ is not allowed, the law of wave vectors conservation being not satisfied. Nevertheless, it can be emphasized that the following coupling term:

$$a_{14} Q(\mathbf{k} = 0)[(e_1 - e_2)e_4 + e_5 e_6] \quad (5)$$

where $Q(\mathbf{k} = 0)$ is the normal coordinate of the $\mathbf{k} = 0$ mode belonging to the soft optical branch is allowed. In the α phase this mode coincides with the soft mode, giving the result:

$$C_{14}^E = a_{14} Q \quad (6)$$

in this phase whereas $C_{14}^E = 0$ in the β phase, as obtained in the earlier consideration. In the incommensurate phase of AlPO_4 , the point symmetry of the β phase being preserved, we have also $C_{14}^E = 0$. These predictions about C_{14}^E at and above T_c are corroborated by the experimental results, as noted in Section 3.3.

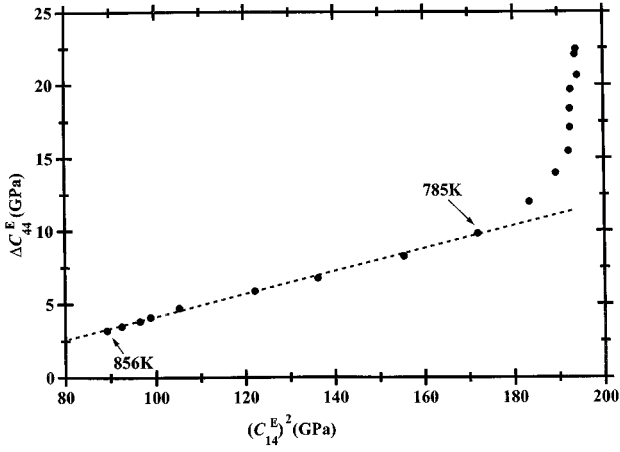
To check the validity of relation (6), we have reported ΔC_{44}^E as function of $(C_{14}^E)^2$ in the α phase (Fig. 6a). Over a temperature range of 70 K below T_c , a linear portion is obtained but its extrapolation does not go through the origin, in conflict with the expectation. To explain this discrepancy we think that it is necessary to put forward higher order coupling terms even near T_c . The next one, allowed by symmetry, can be written as:

$$b_{14} \sum_{\mathbf{k}, \mathbf{k}'} Q(\mathbf{k}) Q(\mathbf{k}') Q(-\mathbf{k} - \mathbf{k}') [(e_1 - e_2)e_4 + e_5 e_6]. \quad (7)$$

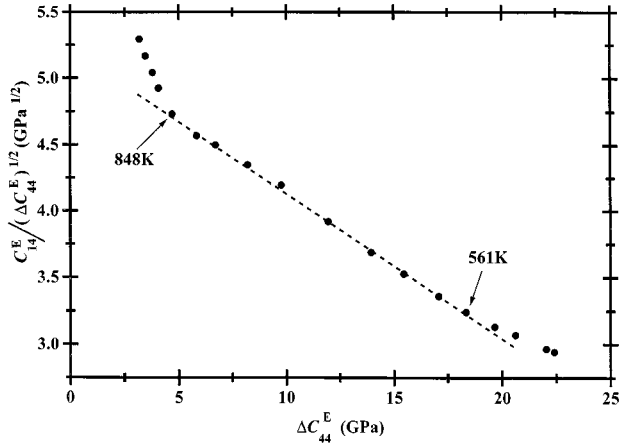
Hence, relation (6) is written as

$$C_{14}^E = a_{14} Q + b_{14} Q^3. \quad (8)$$

Considering that ΔC_{44}^E is proportional to Q^2 over at least 140 K below T_c , as obtained in Section 4.1, relation (8) can be checked by plotting $C_{14}^E / (\Delta C_{44}^E)^{1/2}$ as function of ΔC_{44}^E as shown in Figure 6b. Over ~ 300 K below T_c , a linear part with a negative slope (implying $b_{14} < 0$) is obtained, except in a narrow range of 8 K just below the lock-in transition. This small deviation may be attributed to an additional contribution of coupling (7) coming from fluctuations of $Q(\mathbf{k})$ near $\mathbf{k} = 0$. Then, over about 300 K below T_c , it appears that the experimental results are well fitted by (8), together with (3) for C_{44}^E ; this result also implies that the proportionality of ΔC_{44}^E to Q^2 holds on



(a)



(b)

Fig. 6. (a) Plot of ΔC_{44}^E as function of $(C_{14}^E)^2$ in the α phase. (b) Plot of $C_{14}^E / (\Delta C_{44}^E)^{1/2}$ as function of ΔC_{44}^E in the α phase.

a more extended range than 140 K. An equivalent conclusion has been drawn about C_{14}^E in quartz in which this constant cannot be fitted to others quantities which are expected to be proportional to Q^2 , such as the birefringence variation or a coefficient of second harmonic generation [24]. The progressive deviation from the straight line below 650 K indicates that higher order terms have to be taken into account in (8) and, possibly, in (3).

4.3 Anticrossing in scattering geometries with acoustic wave vector along [010]

The knowledge of $C_{66}^E(T)$, $C_{14}^E(T)$, $C_{44}^E(T)$ and $C_{11}^E(T)$ in the α phase allows a quantitative analysis of the anticrossing which has been observed in scattering geometries 1 and 2. Following the usual procedure, a coupling constant $K = q^2 K'$, reflecting dynamic anharmonic interactions is

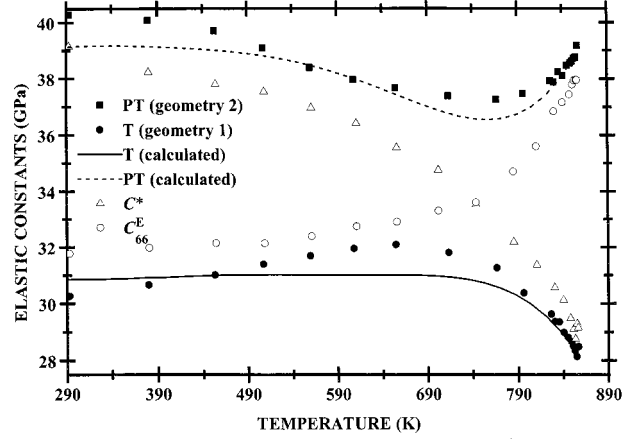


Fig. 7. Plot of experimental and calculated values of ρV_{\pm}^2 and ρV_{\pm}^2 (in scattering geometries 1 and 2) and of calculated C^* and C_{66}^E , in the α phase.

introduced in the eigenvalues equation for the two modes:

$$\begin{vmatrix} C^* - \rho \frac{\omega^2}{q^2} & K \\ K & C_{66}^D - \rho \frac{\omega^2}{q^2} \end{vmatrix} = 0 \quad (9)$$

where $C^* = [C_{11}^E + C_{44}^E - \sqrt{(C_{11}^E - C_{44}^E)^2 + 4(C_{14}^E)^2}] / 2$. The coupling constant K , expressed as $q^2 K'$, reflects a fourth order interaction. It disappears when $\mathbf{q} \rightarrow 0$, preserving the usual set of elastic constants in the static limit. The velocities V_+ and V_- of the coupled modes are given by:

$$\rho V_{\pm}^2 = \frac{C^* + C_{66}^D \pm \sqrt{(C^* - C_{66}^D)^2 + 4K^2}}{2}. \quad (10)$$

The temperature dependences of C_{11}^D and C_{44}^E have been previously measured in the scattering geometries $(-x + y)[z, z](x + y)$ and $(y - z)[x, (y - z)](y + z)$ respectively [6]. Making use of these data, together with the present data on $C_{14}^E(T)$ and $C_{66}^E(T)$ and assuming, in the first approximation, that $C_{11}^E \cong C_{11}^D$ and $C_{66}^E \cong C_{66}^D$, ρV_+^2 and ρV_-^2 have been computed with K as a free parameter, and fitted to experimental results (scattering geometries 1 and 2). The best fit is shown in Figure 7 and corresponds to $K = 3.0 \pm 0.5$ GPa. The agreement between calculated and experimental values can be considered satisfactory, specially near T_c , taking into account (i) the uncertainties on C^* (estimated to 3.5%) and on C_{66}^E and (ii) the assumptions concerning the use of C_{11}^D and C_{66}^E instead of C_{11}^E and C_{66}^D respectively. More precisely, a qualitative analysis of this assumption shows that an increase of C_{66}^E and a decrease of C_{11}^E (to simulate the value of C_{66}^D and the real value of C_{11}^E , respectively) leads to an increase of ρV_-^2 and to an insignificant variation of ρV_+^2 , due to almost cancelling terms. Hence, the fit to experimental results would be improved. The widespread results on the piezoelectric moduli [2–4] prevent a more quantitative analysis.

As conclusion, it can be emphasized that, due to the anticrossing, the scattering geometry 1 is not adequate for

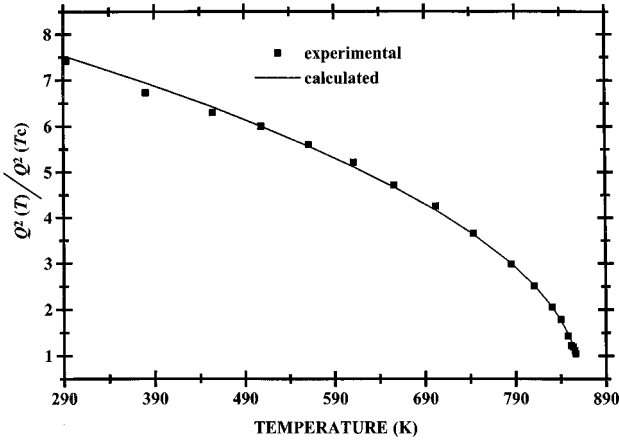


Fig. 8. Temperature dependence of experimental and calculated $Q^2(T)/Q^2(T_c)$.

a precise measurement of C_{66}^D , even at room temperature, as it was anticipated in Section 3.2.

4.4 Temperature dependence of the order parameter

The preceding results, particularly ΔC_{44}^E , allow the determination of the temperature dependence of Q and its comparison to predictions of existing theories. This comparison has been substantially discussed in quartz [24], within the framework of Landau theory and within the renormalization theory by using a power law with a critical exponent $\beta \neq 1/2$. It has been found that $Q(T)$ can be equally fitted to the Landau law and to a power law with $\beta = 1/3$. In that discussion, the transition was considered as an ordinary one, the existence of the incommensurate phase being not known.

In the framework of Landau's theory, incommensurate transitions have been investigated as a special case of continuous structural transitions adjacent to a high-symmetry crystalline phase, with more or less refinements [25]. The various theoretical schemes focus essentially on the specific features of the incommensurate phase. Taking into account only the lowest order terms in the free energy required for the occurrence of a transition, it is generally predicted that, in the locked phase, the order parameter squared varies as $T_0 - T$, with T_0 between T_c and T_i . This law does not fit with our results in AlPO_4 since the extrapolation of the linear part of ΔC_{44}^E , which holds just below T_c , intersects the temperature axis well above T_i (~ 15 K).

This discrepancy may originate in an insufficient number of terms taken into account in the power-series expansion of the free energy with respect to the order parameter. When more than two terms are taken into account, they are known to give a saturation of $Q^2(T)$ on cooling. The presence of the sixth degree term leads to the usual law:

$$Q^2(T) = \frac{-B + \sqrt{B^2 - 4AC}}{2C} \quad (11)$$

where A , B , C are the coefficients of the successive terms with $A = A_0(T - T_0)$, $C > 0$, and $B > 0$ or < 0 for a second or first order transition, respectively. For positive values of B , the experimental results for ΔC_{44}^E cannot be fitted to this law below T_c , with T_0 between T_c and T_i , as a consequence of the large amplitude of the discontinuity at T_c . Therefore, we think that it is necessary to consider that this coefficient would be negative (as in a first order ordinary transition). In this case, from (3) and (11) the following relation can be obtained:

$$\begin{aligned} \Delta C_{44}^E(T)/\Delta C_{44}^E(T_c) &= Q^2(T)/Q^2(T_c) \\ &= \frac{1 + \sqrt{1 + D(T_0 - T)}}{1 + \sqrt{1 + D(T_0 - T_c)}} \end{aligned} \quad (12)$$

where D is a temperature independent constant related to A_0 , B and C ; it is worthy of notice that T_c has not to be identified with the transition temperature T_t which would be associated with T_0 in the case of an ordinary first order transition and, therefore $T_0 < T_c$ is not imposed.

The best fit of experimental results to (12) is obtained for $T_0 = (859 \pm 0.5)$ K and $D = (0.525 \pm 0.005)$ K^{-1} and reported in Figure 8. As can be verified, the temperature dependence of $Q^2(T)$ can be well described by (12), over about 400 K in the α phase, within experimental uncertainty. A similar conclusion has been drawn in quartz [25]. It can be noted that such fits to a Landau law over a large temperature range are always questionable and of small interest; they only give analytical temperature laws which agree with experimental points. As emphasized in this last paper [25], fits to a power law involving a critical exponent are questionable in the case of a first order transition; therefore, such fits have not been undertaken in AlPO_4 .

In the incommensurate phase, no attempt has been made to analyse $Q(T)$. Different types of difficulties arise, among which (i) the narrowness of its temperature range, (ii) the fact that several contributions are likely added in ΔC_{44}^E .

5 Conclusion

The present Brillouin investigation reports, for the first time in AlPO_4 , a study of the transverse and pseudo-transverse elastic waves in several scattering geometries over the temperature range 300 K-1100 K. These scattering geometries allow the determination of the temperature dependences of C_{66}^E and C_{14}^E which completes that of C_{44}^E , already reported in one of our previous work. The analysis of the results has shown that the lowest order coupling term between strains and order parameter is sufficient to account for the anomaly of C_{44}^E in a large temperature range below T_c (at least 300 K), whereas additional coupling term(s) have to be taken into account in the case of C_{66}^E at temperature lower than 140 K below T_c , reflecting a greater anharmonicity for that constant. In the case of C_{14}^E , the first two lowest order terms must be taken into account even just below T_c . Such a detailed analysis has never been performed in quartz. However, taking into

account the similarity of experimental data about elastic constants in AlPO_4 and quartz, when available, it is likely that the same conclusions also hold in this last material. In AlPO_4 , our data also allow the determination of the order parameter temperature dependence in the α phase, which can be successfully described within the framework of Landau's theory.

All these results, which have been obtained from significant pretransitional features occurring over a large temperature range around the α - β transition, show that compounds such as AlPO_4 and, more generally quartz-like materials, yield an important investigation field of the anharmonicity in a solid. Some of their properties still remain not understood as, for example, the anomalous increase of some bare elastic constants on heating, as can be directly observed in the β phase.

References

1. K. Kosten, H. Arnold, Z. Krist. **152**, 119 (1980).
2. Z.P. Chang, G.R. Barch, IEEE Trans. Sonics and Ultrasonics **23**, 127 (1976).
3. D.S. Bailey, J.C. Andle, D.L. Lee, W. Soluch, J.F. Veletino, Proc. of the 1983 IEEE Ultrasonic Symp. (1983) p. 335.
4. I.M. Sil'Vestrova, Yu. V. Pisarevskii, O.V. Zvereva, A.A. Schternberg, Sov. Phys. Crystallogr. **32**, 467 (1987).
5. C. Ecolivet, H. Poignant, Phys. Status Sol. (a) **63**, K107 (1981).
6. N. Magneron, Y. Luspin, G. Hauret, E. Philippot, J. Phys. I France **7**, 569 (1997).
7. H.E. Swanson, M.I. Cook, E.H. Evans, J.H. de Groot, in *Standard X-Ray Diffraction Powder Pattern*, Nat. Bur. Standards (U.S.) Circ. 539, **10**, 3 (1960).
8. S.M. Shapiro, H.Z. Cummins, Phys. Rev. Lett. **21**, 1578 (1968).
9. O.A. Shustin, T.G. Chervitch, S. Ivanov, Sol. State Commun. **37**, 65 (1981).
10. G. Van Tendeloo, J. Van Landuyt, S. Amelinckx, Phys. Status Sol. (a) **33**, 723 (1976).
11. J.P. Bachheimer, B. Bergé, G. Dolino, Solid State Commun. **51**, 55 (1984).
12. J.V. Atanasoff, P.J. Hart, Phys. Rev. **59**, 85 (1941).
13. U.T. Höchli, Solid State Commun. **8**, 1487 (1970).
14. V.G. Zubov, M.M. Firsova, Sov. Phys. Crystallogr. **7**, 374 (1962).
15. S. Ishibashi, K. Abe, M. Suzuki, Y. Sasaki, Physica B **219&220**, 593 (1996).
16. E.W. Kammer, T.E. Pardue, H.F. Frissel, J. Appl. Phys. **19**, 265 (1948).
17. B. Bergé, G. Dolino, M. Vallade, M. Boissier, R. Vacher, J. Phys. France **45**, 715 (1984).
18. U.T. Höchli, J.F. Scott, Phys. Rev. Lett. **26**, 1627 (1971).
19. W. Rehwald, Adv. Phys. **22**, 721 (1973).
20. T.A. Aslanyan, A.P. Levanyuk, M. Vallade, J. Lajzerowicz, J. Phys. C **16**, 6705 (1983).
21. Y. Luspin, G. Hauret, A.M. Gillet, Ferroelectrics **65**, 1 (1985).
22. G. Dolino, J.P. Bachheimer, B. Bergé, C.M.E. Zeyen, J. Phys. France **45**, 361 (1984).
23. J.D. Axe, G. Shirane, Phys. Rev. B **1**, 342 (1970).
24. J.P. Bachheimer, G. Dolino, Phys. Rev. B **11**, 3195 (1975).
25. J.C. Toledano, P. Toledano, *The Landau theory of phase transitions* (World Scientific, Singapor, New Jersey, Hong Kong, 1987).